Early postnatal exposure to lithium *in vitro* induces changes in AMPAR mEPSCs and vesicular recycling at hippocampal glutamatergic synapses

SHREYA M ANKOLEKAR and SUJIT K SIKDAR*

Molecular Biophysics Unit, Indian Institute of Science, Bangalore 560 012, India

**Corresponding author (Fax, 91(080) 23600535; Email, sks@mbu.iisc.ernet.in)*

Lithium is an effective mood stabilizer but its use is associated with many side effects. Electrophysiological recordings of miniature excitatory postsynaptic currents (mEPSCs) mediated by glutamate receptor AMPA-subtype (AMPARs) in hippocampal pyramidal neurons revealed that CLi (therapeutic concentration of 1 mM lithium, from days *in vitro* 4–10) decreased the mean amplitude and mean rectification index (RI) of AMPAR mEPSCs. Lowered mean RI indicate that contribution of Ca^{2+}-permeable AMPARs in synaptic events is higher in CLi neurons (supported by experiments sensitive to Ca^{2+}-permeable AMPAR modulation). Co-inhibiting PKA, GSK-3β and glutamate reuptake was necessary to bring about changes in AMPAR mEPSCs similar to that seen in CLi neurons. FM1-43 experiments revealed that recycling pool size was affected in CLi cultures. Results from minimum loading, chlorpromazine treatment and hyperosmotic treatment experiments indicate that endocytosis in CLi is affected while not much difference is seen in modes of exocytosis. CLi cultures did not show the high KCl associated presynaptic potentiation observed in control cultures. This study, by calling attention to long-term lithium-exposure-induced synaptic changes, might have implications in understanding the side effects such as CNS complications occurring in perinatally exposed babies and cognitive dulling seen in patients on lithium treatment.

[Ankolekar SM and Sikdar SK 2015 Early postnatal exposure to lithium *in vitro* induces changes in AMPAR mEPSCs and vesicular recycling at hippocampal glutamatergic synapses. *J. Biosci.* **40** 339–354] **DOI** 10.1007/s12038-015-9527-3

1. Introduction

Glutamatergic synapses are emerging as the focus of studies on genesis and treatment of mood disorders (Kugaya and Sanacora 2005). Glutamatergic system is dysfunctional in mood disorder patients and many antidepressants and mood stabilizers have been shown to modulate glutamatergic transmission (Kugaya and Sanacora 2005). Lithium too has been shown to modify glutamatergic transmission. Study of long-term exposure to lithium at the therapeutic concentrations (1 mM) has revealed that phosphorylation level of GluN2B is affected by chronic exposure to lithium, which leads to lower Ca^{2+} influx through NMDAR (Hashimoto *et al.* 2002). Chronic exposure to lithium has also been

Keywords. AMPARs; FM1-43; hippocampal glutamatergic synapses; lithium side effects; mEPSCs; rectification index; synaptic recycling

Abbreviations used: AMPARs, α-amino-3-hydroxy-5-methyl-4-isoxazolepropionate receptors; CLi, long-term lithium-treated cultures; DFMO, Di-fluoro-methyl-ornithine; GSK-3β, glycogen synthase kinase-3β; I-V curve, current–voltage curve; mEPSCs, miniature excitatory postsynaptic currents; NASPM, *N*-acetyl spermine; NMDARs, *N*-methyl-D-aspartate receptors; P in P0, P2 and P8, postnatal day; PKC, protein kinase C; RI, rectification index; RP, reserve pool; RRP, readily releasable pool

Supplementary materials pertaining to this article are available on the *Journal of Biosciences* Website at *http://www.ias.ac.in/jbiosci/jun2015/supp/Ankolekar.pdf*

Published online: 27 April 2015

shown to bring down the surface expression of GluA1/GluA2 AMPARs in hippocampal neuronal cultures (Du *et al.* 2008). However, most of these studies have focused on mature synapses (treatment started from days *in vitro* (DIV) > 8 for hippocampal cultures from P0–P2 pups and DIV 1/2 for cultures obtained from P8 and above pups).

Studies on long-term exposure to lithium on synapse formation are very few. Lithium brings about adult neurogenesis in hippocampus and this is thought to be one of the reasons for its effectiveness in prophylaxis (Chen *et al.* 2000; Manji *et al.* 2001). One of the major side effects seen in patients on lithium is cognitive disability (Dunner 2000). It becomes important to study the effect of lithium on developing synapses. Another reason for studying its effect on developing synapses is the CNS complications reported in babies born of mothers on lithium therapy who are perinatally/neonatally exposed to lithium (Newport *et al.* 2005). Lithium modulates many second messengers which are also involved in synapse formation (Phiel and Klein 2001; Lenox and Wang 2003; Bonanomi *et al.* 2005; Speese and Budnik 2007; Akaneya *et al.* 2010).

Synaptogenesis begins by DIV 4 in culture (Cottrell *et al.* 2000). AMPAR and NMDAR are expressed in the neurons by DIV 3 (van den Pol *et al.* 1998). Presynaptic terminals are also present by DIV 4 (van den Pol *et al.* 1998). Accelerated coupling between presynapse and postsynapse occurs during DIV 8-10. The development of synapses during the postnatal 2 weeks in rodents and the development of synapses in babies during the last trimester to 3 years of age are similar (Loepke *et al.* 2008). Many parallels can be drawn in the development of synapses in adult brain and that happening in culture (Cohen-Cory 2002). Therefore, using hippocampal neuronal cultures as a model system, electrophysiology and FM1-43 as experimental tools, the effect of lithium exposure (therapeutic concentration, 1 mM, DIV 4-10), on expression of synaptic AMPARs and vesicular recycling, has been studied.

It was found that such a lithium treatment brings down the AMPAR mEPSC amplitude, lowers rectification index (RI) and impairs vesicular recycling. It also impairs presynaptic high KCl-associated potentiation. This study could have implications in understanding the cognitive disabilities in patients and CNS complications in perinatally lithium exposed babies when mothers are on lithium treatment.

2. Materials and methods

2.1 *Culturing hippocampal neurons and lithium treatment protocol*

Hippocampal neuronal cultures were obtained using the method used earlier in the lab (Rao and Sikdar 2004; Srinivas *et al.* 2007). Briefly, hippocampii isolated from P0-P2 day old Wistar rat pups were treated with papain solution (20 U/mL enzyme activity at 25°C) for 30 min and then washed with culture medium. They were then mechanically dissociated by trituration and filtered through a nylon mesh. The filtered homogenate was then spun in a centrifuge at 1000*g* for 5 min, the supernatant discarded and the pellet resuspended in culture medium. The single cell suspension was then seeded directly onto culture dishes or on PEI coated coverslips (for FM1-43 experiments) at cell density of 1×10^3 cells/mm^3. After an initial adherence period of 1 h, at 37°C in a humidified incubator supplied with 5% CO_2, 2 mL culture media was added to the culture dish. The neurons were then maintained in the humidified incubator supplied with 5% CO_2 at 37°C. One-half of the medium was changed every 3 days. The culture medium contained DMEM F12 HAM with 1% N-1 supplement, 10% FBS (Invitrogen) and 1% antibiotic-antimycotic (Invitrogen). 10 μM Cytosine β-D arabinofuranoside (Ara-C) was added after few days in culture to avoid astrocyte overgrowth. The neuronal cultures were viable for 15–16 days when grown this way. The lithium treatment protocol used for our studies was similar to the one used earlier (Nonaka *et al.* 1998; Hashimoto *et al.* 2002) with slight modification. Lithium chloride, final concentration 1 mM, was added to 4 days old cultures (DIV 4) and the treatment was carried out for the next 6 days. Such cultures were termed as chronic lithium-treated cultures (CLi). Care was taken to minimize the animal suffering and the number of animals used; the experiments done were approved by the institute ethical committee. All products and chemicals used in this study are from Sigma unless mentioned otherwise.

2.2 *Electrophysiology*

2.2.1 *Recording AMPAR mEPSCs:* Whole cell recordings were done in voltage clamp mode on randomly picked pyramidal shaped neurons in 10–15 days old hippocampal cultures under control and CLi treatment conditions mentioned above. Thin-walled borosilicate glass capillaries with filament (Harvard Apparatus Ltd., USA) were pulled using P-97 Flaming/Brown micropipette puller (Sutter Instrument Company, USA). Pipette tips were fire polished. Pipette resistance was between 4–7 MΩ. For recording spontaneous miniature excitatory postsynaptic currents (mEPSCs) mediated by AMPARs, the external solution had (in mM): 145 NaCl, 2.5 KCl, 1 $MgCl_2$, 2 $CaCl_2$, 10 HEPES and 10 glucose. 1 μM TTX, 100 μM DL-APV and 50 μM Picrotoxin were also added to the external solution. Final external solution had a pH of 7.4 and osmolarity lay within the range of 290–300 mOsm. Internal solution had (in mM): 115 potassium gluconate, 20 KCl, 2 EGTA, 4 Mg-

ATP, 0.3 Na-GTP and 10 HEPES (pH 7.3). EPC-8 amplifier (HEKA, Germany), Digidata (1320A, Axon Instruments Inc., USA) and Clampex software (Axon Instruments Inc., USA) were used. All experiments were carried out at 23-25°C. Series resistance compensation of 70% was used. For obtaining the I-V curve and rectification indices, the neurons were held at different holding potentials (V_H) ranging from −70 mV to +50 mV and the mEPSCs mediated by the AMPARs (called AMPAR mEPSCs henceforth) were measured in gap free mode in voltage clamp configuration. E_{rev} obtained from I-V plots was around 0 mV (it varied from −2.5 to 2.5 mV). Rectification index, RI, was estimated using the equation given below (Kamboj *et al.* 1995, Yang *et al.* 2008), (the averaged AMPAR mEPSC amplitudes at a given voltage were used)

$$RI = [I_{+50}/(+50-E_{rev})/\ I_{-70}/(-70-E_{rev})] \quad \text{(i)}$$

where I_{+50} is the averaged mEPSC amplitude at +50 mV; I_{-70}, averaged mEPSC amplitude at −70 mV; and E_{rev}, reversal potential.

2.2.2 *Data analysis and statistical tests:* AMPAR mEPSCs were analysed using MiniAnalysis Program (Version 6.0.1, Synaptosoft Inc.) and the events were selected manually. Mean amplitudes and rectification indices were calculated using Sigma Plot software (SPSS Inc, USA). Kinetic parameters were calculated from normalized events; τ_{decay} was obtained by monoexponential fits using MiniAnalysis and Sigma Plot softwares. The number of neurons and the events in each treatment class has been mentioned in the legend and result section. Data have been averaged and shown as mean±standard error of mean (SEM). GraphPad software (GraphPad Software Inc, USA) was used for statistical tests and $p<0.05$ defined a significant difference while $p>0.05$ defined an insignificant difference. The relevant tests used and their outcomes have been mentioned in the appropriate places in the results section or figure legend.

2.3 *FM1-43 experiments*

2.3.1 *Loading and destaining protocol:* Hippocampal neuronal cultures (DIV 11-15) grown on PEI-coated glass coverslips were used for FM1-43 experiments. High KCl modified tyrode solutions (MT) were used for loading and destaining. The normal external solution contained (in mM) 119 NaCl, 2.5 KCl, 2 $MgCl_2$, 2 $CaCl_2$, 25 HEPES and 10 glucose. It also contained (in μM) 1 TTX, 10 CNQX, 100 DL-APV and 50 picrotoxin. The pH of the solution was 7.4 and osmolarity lay between 290–300 mOsm. When preparing high KCl solutions, equimolar NaCl was substituted (Sara *et al.* 2002). The 90 mM KCl MT contained (in mM): 90 KCl, 31.5 NaCl, 2 $CaCl_2$, 2 $MgCl_2$, 25 HEPES and 10 glucose. 1μM TTX, 10μM CNQX, 100 μM DL-APV, 50 μM picrotoxin were also included. Final solution had pH 7.4 and osmolarity between 290–300 mOsm. MT with 12 mM KCl and 25 mM KCl were also used in some experiments with appropriate changes in NaCl concentration. Hyperosmotic solutions were prepared by addition of sucrose; 800 mOsm solutions were made by adding 500 mM sucrose to normal external solution (Sara *et al.* 2002). For loading, the cultures were depolarized in the presence of 10 μM FM1-43 dye (*N*-(3-triethylammoniumpropyl)-4-(4-(dibutylamino) styryl) pyridinium dibromide; Molecular Probes) for 60 seconds and then washed thoroughly with normal external solution containing 1 mM Advasep-7. Destaining during imaging was brought about by perfusing high KCl MT solution. The solutions were perfused at a rate of 1 mL/min using a Gilson peristaltic pump (MP3, Gilson, France).

2.3.2 *Imaging and data analysis:* Fluorescence imaging was done using a cooled CCD camera (CoolSnap fx, Photometrics, USA) attached to a Nikon inverted microscope (Nikon Diaphot TMD) using a 60× plan apochromat oil immersion objective lens. Excitation was at 488 nm and emission was at 520 nm. Similar settings of monochromatic light intensity were used to illuminate the samples in all experiments. Images were acquired at a rate of 1 image per 310 ms for all experiments, excepting minimum loading experiment. For minimum loading experiment the images were acquired at a rate of 1 image per 2.3 s. Metafluor (Universal Imaging, USA) was used to acquire and store data. Regions of interest (ROIs) were picked and fluorescence values were extracted using Metavue (Universal Imaging, USA). Bleach was estimated by linearly fitting the fluorescence of the 15 images (last 5 s) at the end of the destaining period and corrected for (bleach was <1 % per image) (Wierenga *et al.* 2005). The change in fluorescence (ΔF) in the regions of interest was calculated as the difference in fluorescence seen before depolarization, baseline period (Fo) and that seen 80 s from start of stimulation (F) and normalized with respect to Fo and represented as percentage change in fluorescence (% ΔF/F). Exponential decay fits were used to obtain the destaining rate constants, τ (SigmaPlot). Post bleach correction, the decay part of the fluorescence profile could be fit with a biexponential equation of the form given below

$$y = y_o + ae^{-b*\,x} + ce^{-d*\,x} \quad \text{(ii)}$$

Inverse of the parameters 'b' and 'd' gave the two τ values (τ_{fast} and τ_{slow}). Paramters 'a' and 'c' gave the associated amplitudes.

Data analysis was done in Excel sheets; statistical analysis was done using GraphPad. Unpaired two-tailed *t*-test was used to check for significance, $p<0.05$ was taken as significant. Averaged data have been shown as mean±standard error of mean (mean±SEM).

3. Results

3.1 *Characterization of AMPAR-mediated mEPSCs reveals a decrease in amplitude and rectification index of AMPARs upon chronic lithium treatment*

AMPAR mediated mEPSCs from pyramidal shaped neurons in dissociated hippocampal neuronal cultures were recorded at different holding voltages (−70 mV to +50 mV). Sample traces and the I-V plots are shown in figure 1A–C. The amplitudes at both +50 mV and −70 mV were significantly smaller in CLi neurons than that of control. The mean amplitude of the AMPAR mediated mEPSCs at −70 mV and +50 mV for control neurons was −27.09±0.74 and +44.11±0.73 (pA) and for CLi neurons was −23.88±0.63 and +30.92±0.41 (pA) respectively (figure 1D).

AMPARs differ in their Ca^{2+}-permeabilities depending on subunit composition. Ca^{2+}-impermeable AMPARs are resilient to the block by internal polyamines such as spermine. Ca^{2+}-permeable AMPARs on the other hand are susceptible to such a block (Shin *et al.* 2005). The block by polyamines is voltage dependent, i.e. the block increases at positive membrane potentials (Shin *et al.* 2005). Thus Ca^{2+}-permeable AMPARs conduct less at positive membrane voltages than at more negative voltages. This is usually quantified by estimating the RI which is calculated as the ratio of amplitudes observed at positive holding voltage to the amplitudes observed at negative holding voltage for the same neuron (equation (i)). The mean RI for control was 1.75±0.16 and that for CLi was 1.29±0.09 (figure 1E), which indicate that the event amplitudes at +50 mV of chronic lithium-treated neurons were significantly affected as compared to −70mV.

The AMPAR mEPSC half rise time and decay time of CLi were not significantly different than that seen in control. The mean half rise time (obtained from normalized events at −70 mV) in control was (in ms) 0.83±0.06 while that in CLi neurons was 0.75±0.07 (figure 2B). The τ_{decay} for control was (in ms) 3.62±0.44 and for CLi neurons, 2.77±0.19 (figure 2C). The control frequency, 0.59±0.14 Hz, was not significantly different from that of CLi neurons, 1.28 ±0.41 Hz (figure 2D).

The reduction in mean RI of neurons seen upon chronic lithium treatment could be due to several reasons -the differences in contribution from space clamp and dendritic filtering, increase in contribution of Ca^{2+}-permeable AMPARs to the synaptic events, or increase in the levels of intrinsic polyamines (Kamboj *et al.* 1995, Liu *et al.* 2006). The plots of half rise-time-amplitude and half rise-time- tau decay plots did not reveal any significant differences in space-clamp or dendritic filtering properties of the neurons in control and CLi cultures (supplementary figures 1.1 and 1.2). A series of experiments were then performed – NASPM bath application, DFMO treatment and spermine inclusion – to elucidate the decrease in mean RI seen in CLi neurons.

3.2 *Effect of NASPM bath inclusion, DFMO treatment and spermine inclusion in internal solution on mean RI of AMPARs in Control and CLi cultures*

The synthetic analogue of Joro spider toxin (JSTX) (Koike *et al.* 1997), N-Acetyl Spermine (NASPM, 20 μM), a Ca^{2+}-permeable AMPAR blocker was included in the external bath solution to see if its presence had any effect on the mean RI of control and CLi neurons. The block by NASPM is voltage sensitive, it is relieved above +40mV. Ca^{2+}-permeable AMPARs would be blocked at −70 mV and the block would be relieved at +50 mV, affecting the denominator in equation (i) while leaving the numerator unaffected. Thus in the presence of NASPM a higher mean RI in CLi is expected if there is an increase in the relative density of Ca^{2+}-permeable AMPARs associated with the treatment. In the presence of this selective Ca^{2+}-permeable AMPAR blocker, we found that the mean RI of chronic lithium-treated pyramidal neurons showed a significant increase (1.77±0.17) (n=13) (figure 3D). The mean RI of control pyramidal neurons showed an increase but the increase was not significant (1.98±0.21) (n=21) (figure 3D). In the presence of NASPM the mean RI of CLi neurons showed a 1.47 fold increase, while that of control neurons increased only by 1.13 times (figure 3G). Thus, the effect of NASPM seen here may be interpreted as an increase in the proportion of Ca^{2+} permeable AMPARs which contribute to the synaptic events in CLi neurons.

Di-fluoro-methyl-ornithine, DFMO, is an inhibitor of Ornithine Decarboxylase, the enzyme responsible for polyamine synthesis (Shin *et al.* 2005). Thus, DFMO acts to remove the source of polyamine block responsible for the decrease in outward conductance in Ca^{2+}-permeable AMPA Rs and thus relieves the rectifying property. In the absence of polyamines, therefore a reversal of RI associated with an increase in Ca^{2+}-permeable AMPARs is expected. We found that two hour incubation with 1 mM DFMO was enough to reverse the decrease in RI seen in chronic lithium-treated neurons. . The RI of chronic lithium-treated neurons increased by about 1.53 times (mean RI for CLi + DFMO 1.97±0.23,(n=13) (figure 3E) whereas that of control neurons increased by about 1.29 times (figure 3G), (mean RI for Control + DFMO 2.26±0.32, (n=9) (figure 3E).The significant increase in RI after DFMO treatment in CLi thus indicates that there is an increase in the contribution from Ca^{2+}-permeable AMPARs.

Polyamines are known to be modulated under several physiological conditions and as they are involved in many cell processes their modulation is physiologically important (Iqbal 1995). Effect of lithium treatment on ploymine levels

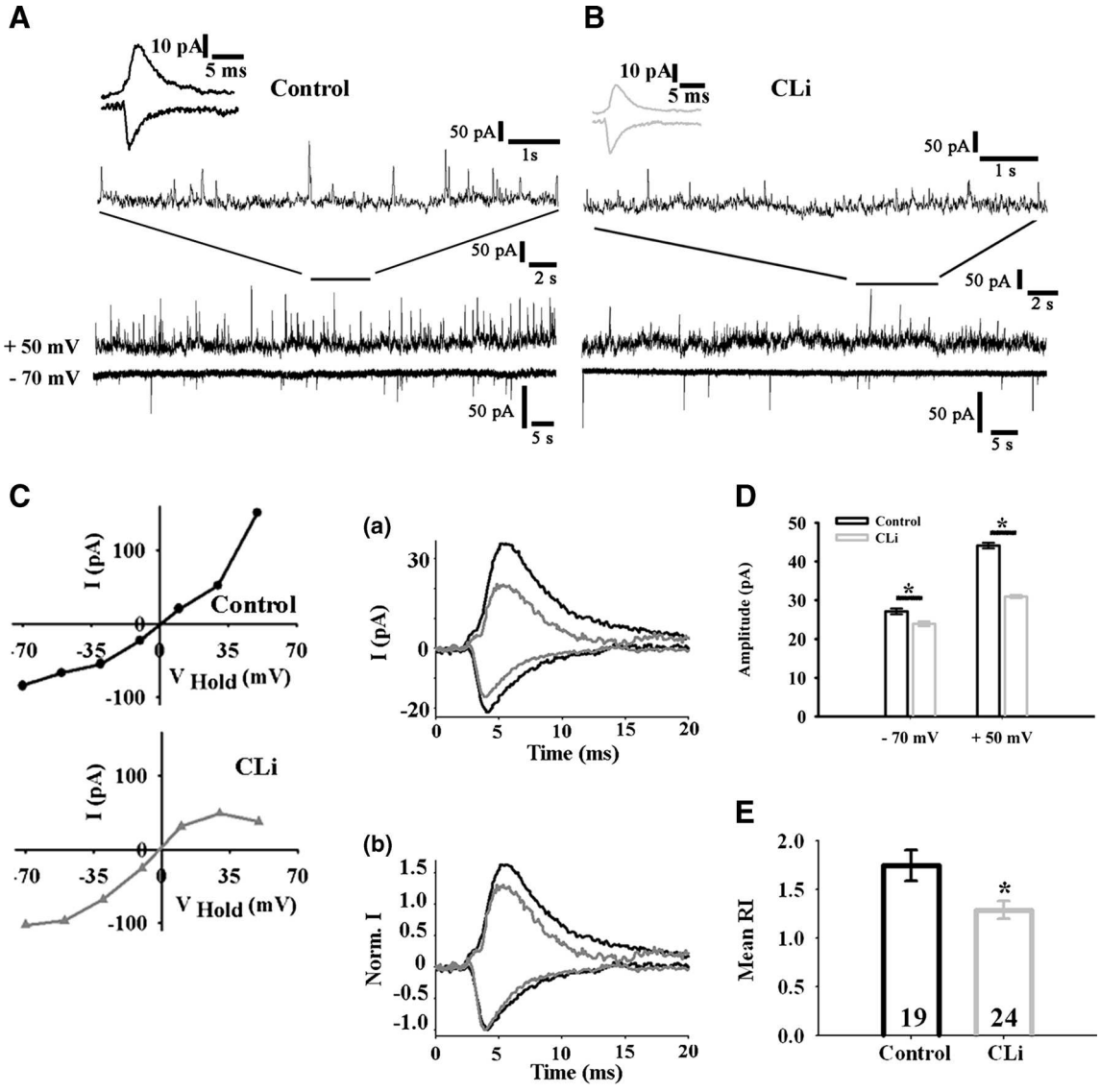

Figure 1. Lithium-treated hippocampal pyramidal neurons in culture show decreased AMPAR mEPSC amplitude and rectification index. (**A**) Sample raw traces of the AMPAR mediated mEPSCs recorded (in presence of TTX, APV and Picrotoxin in voltage clamp gap-free mode) at +50 and −70 mV holding voltages in control and (**B**) CLi (1 mM LiCl from DIV 4 for 6 days); the relevant sections from the recordings at +50 mV are indicated above the current trace at +50 mV. Insets (**A**) and (**B**) show averaged mEPSC for the recordings, (**C**) sample I-V relationship of mEPSCs in control and CLi; (**C(a)**) Overlay of averaged AMPAR mEPSC traces for control (black) and CLi (grey) at the two holding voltages for recordings shown in (**A**) and (**B**), (**C(b)**) Overlay of the normalized AMPAR mEPSC trace for the traces shown in (**C(a)**) (Trace normalized with respect to I_{max} value of the averaged mEPSC at −70 mV where I is the current amplitude); (**D**) CLi significantly reduces the mean amplitude of AMPAR mEPSCs in pyramidal neurons of hippocampal cultures (control – 723 events and CLi – 829 events at −70 mV and control – 1098 events and CLi – 1415 events at +50 mV) (only magnitudes of mEPSC at −70mV and +50 mV represented, without the respective signs, for easy comparison) ; (**E**) Mean rectification index (RI) of CLi and control neurons, (numbers inside the bars indicate the number of neurons in each group) (*significant at $p<0.05$, unpaired two-tailed *t*-test).

is not clear (Sjöholm *et al.* 1992; Gilad *et al.* 1994; Sparapani *et al.* 1997; Gilad and Gilad 2007). To test the possibility of increase in levels of intrinsic polyamines upon lithium treatment (without change in receptor sub type), we included spermine in the internal solution during whole cell recording of AMPAR mediated spontaneous mEPSCs in control condition. We found that inclusion of spermine had no significant effect on the mean RI (figure 3F). Mean RI of control with spermine at beginning of recording was 1.65 ±0.25, mean RI of control with spermine after 15 minutes

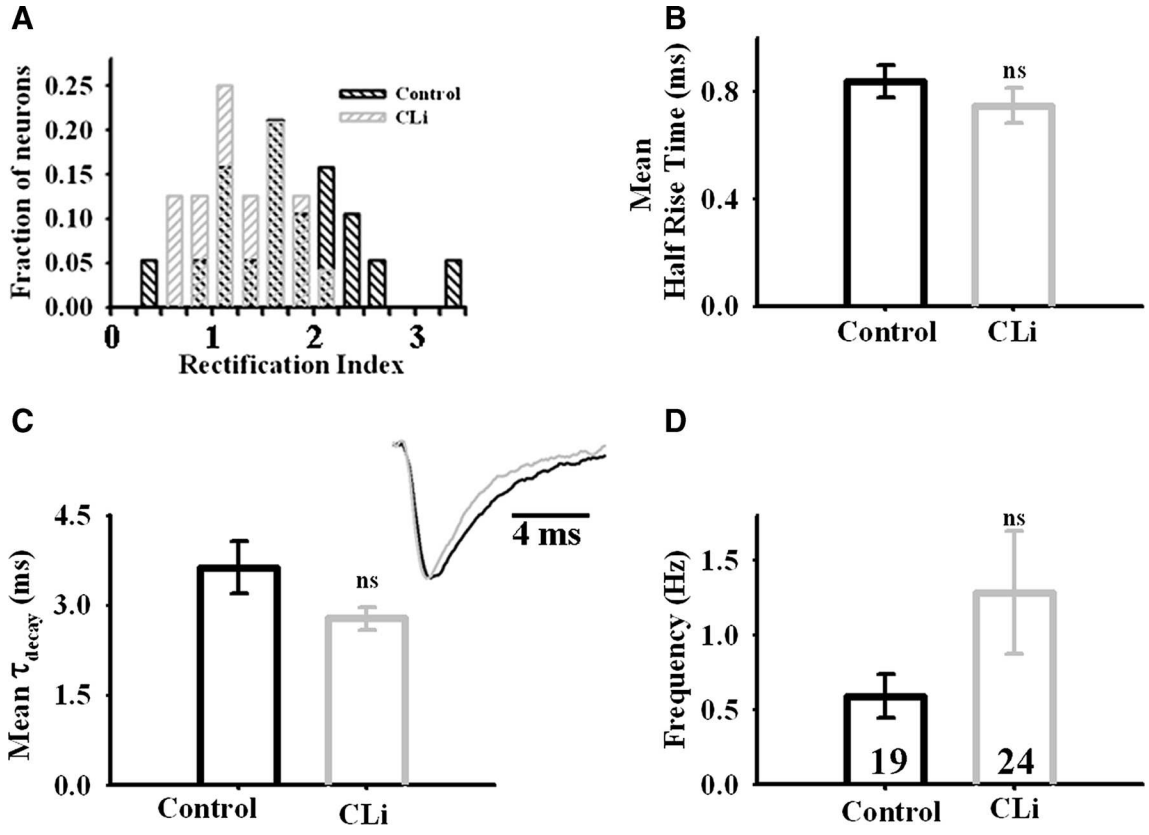

Figure 2. The kinetics of AMPAR mEPSCs and the frequency are not affected by lithium treatment. (**A**) Histogram of rectification indices of neurons in control and CLi cultures; (**B**) the rise time of mEPSCs as well as (**C**) the decay time are not significantly different in CLi-treated neurons; (inset in **C**) overlaid traces of normalized average AMPAR mEPSCs in control and CLi neurons (black trace for control and gray for CLi); (**D**) the mEPSC frequency is not significantly different in the CLi neurons (*significant at $p<0.05$ and ns (non-significant) at $p>0.05$ unpaired two-tailed *t*-test).

was 1.67±0.25 (n=8), mean RI of CLi neurons with spermine at beginning of recording was 1.14±0.19 and mean RI of CLi neurons with spermine after 15 minutes was 1.19 ±0.25 (n=6). Failure to observe a decrease in mean RI in control neurons in the presence of spermine suggest that increased levels of intrinsic polyamines is not responsible for the decreased RI upon lithium treatment.

The slight increase in mean RI of control neurons, with DFMO treatment and in the presence of NASPM, expressed as relative increase in RI (figure 3G), could indicate that there is a minor contribution from Ca^{2+}-permeable AMPARs to the synaptic events in control conditions. It has been reported earlier that distal dendrites of the hippocampal pyramidal neurons do show the presence of Ca^{2+}-permeable AMPARs (Ogoshi and Weis 2003). The AMPAR mEPSCs as indicated by the change in mean RI in CLi cultures were however more sensitive to NASPM and DFMO treatments (figure 3G).

To summarize, bath application of NASPM caused a reversal of mean RI in the case of CLi neurons (figure 3D). Following treatment with DFMO, mean RI of CLi neurons reversed (figure 3E). Experiments with inclusion of spermine did not lead to a decrease in the mean RI of controls (figure 3F). From the above observations, we can conclude that (a) CLi treatment might be affecting the synaptic expression of the AMPARs and (b) the contribution of Ca^{2+}-permeable AMPARs to the synaptic events seems to be higher in CLi-treated neurons as reflected in the RI changes.

3.3 *FM1-43 dye loading and kinetics of unloading are affected in lithium-treated cultures*

Effect of prolonged lithium exposure on vesicular release in developing synapses has not been reported. In this study the effect of lithium exposure, at therapeutically relevant concentration (1 mM, given from DIV 4 for 6 days, during synapse development phase, CLi) on the vesicular release was studied. The synapses in hippocampal neurons contain a readily releasable pool (RRP), reserve pool (RP) and a

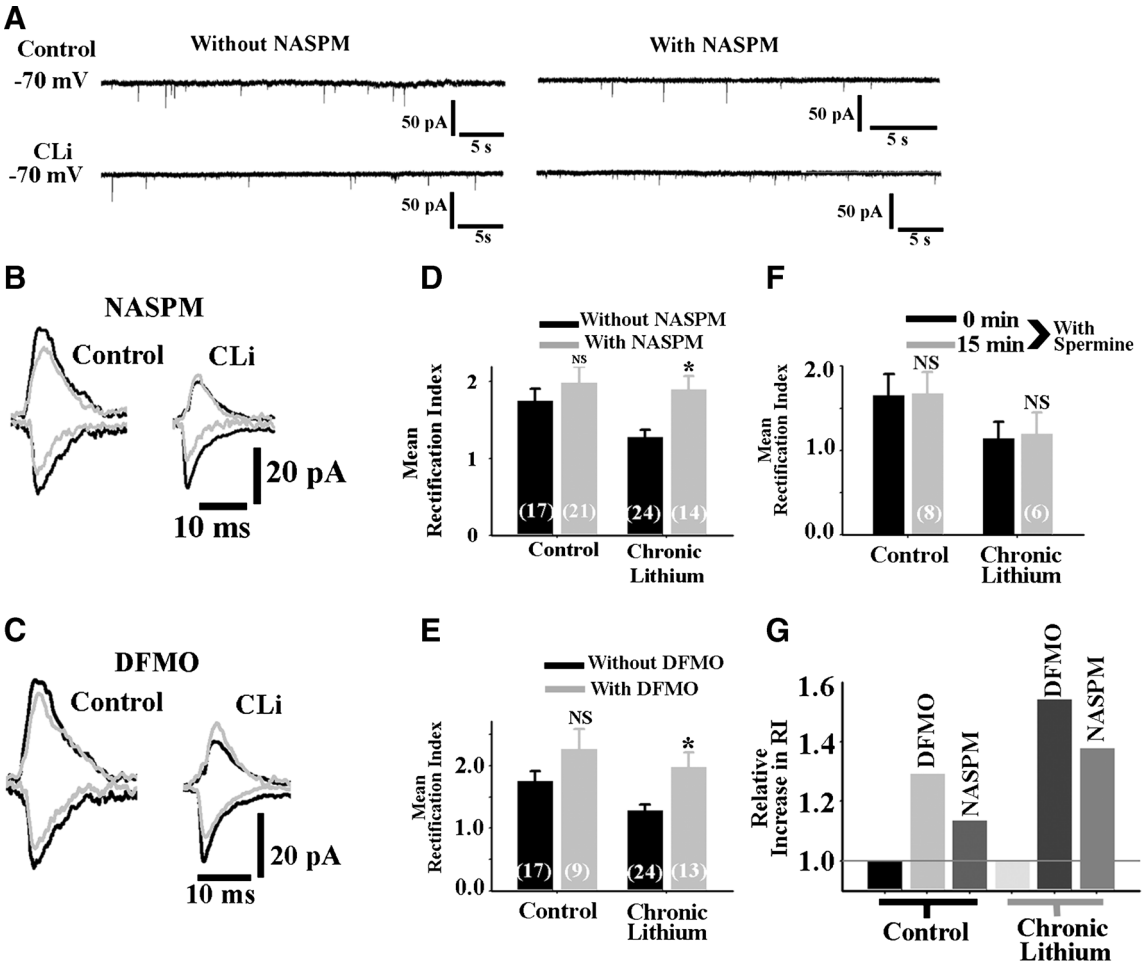

Figure 3. Events in CLi neurons are more sensitive to treatments which specifically affect Ca^{2+}-permeable AMPARs. (**A**, **B** and **D**) results from NASPM experiments are shown; (**A**) recordings of AMPAR mEPSCs with and without NASPM in the bath for control and CLi neurons; (**B**) averaged events at −70 mV and +50mV for control and CLi overlapped with averaged events in presence of 20μM NASPM (black lines – without NASPM and grey lines - with NASPM); (**D**) increase in mean RI upon bath application of 20 μM NASPM in control and chronic lithium-treated neurons; (**C** and **E**) results from DFMO experiments; C] averaged events at −70 mV and +50mV for control and CLi overlapped with averaged events after treatment (black lines – without DFMO and grey lines – with DFMO treatments); (**E**) mean RI is significantly increased in CLi after 2 h treatment with 1 mM DFMO (at 37°C), whereas the increase is non-significant for control; (**F**) inclusion of spermine (100 μM) in internal solution has no significant effect on the mean RI in the two conditions: control with spermine and CLi with spermine; (**G**) effect of DFMO and NASPM on the reversal of mean RI of control and CLi represented as a relative increase after treatment with them (*indicates $p<0.05$ and NS indicates $p>0.05$ with unpaired *t*-test; numbers inside the bars indicate the number of neurons in each group).

resting pool. RRP and RP pool make up the recycling pool. To assess the vesicles in recycling pool for control and CLi, boutons in cultures were loaded with 10 μM FM1-43 with a 90 mM KCl MT stimulus given for 1 min (this loading will be referred to as vesicular recycling I (Recyc I)). After a thorough wash period of 10 min with 1 mM Advasep−7 they were destained with a second destaining 90 mM KCl MT pulse.

The fluorescence intensities (in arbitrary units (a.u.)) obtained post loading were 145.01±1.27 for control and 134.94 ±1.21 for CLi boutons, significantly lower than control (figure 4D). With the destaining pulse, the % destaining seen in control was 21.70±0.27 and that for CLi was 20.78±0.33, significantly different from control destaining (figure 4E. The destaining profiles could be fit with biexponential curve (equation (ii)) giving two time constants τ_{fast} and τ_{slow} (figure 4F), which has been shown to be typical of mature synapses (hippocampal cultures, DIV 10 and above) (Mozhayeva *et al.* 2002). For control, the mean τ_{fast} was

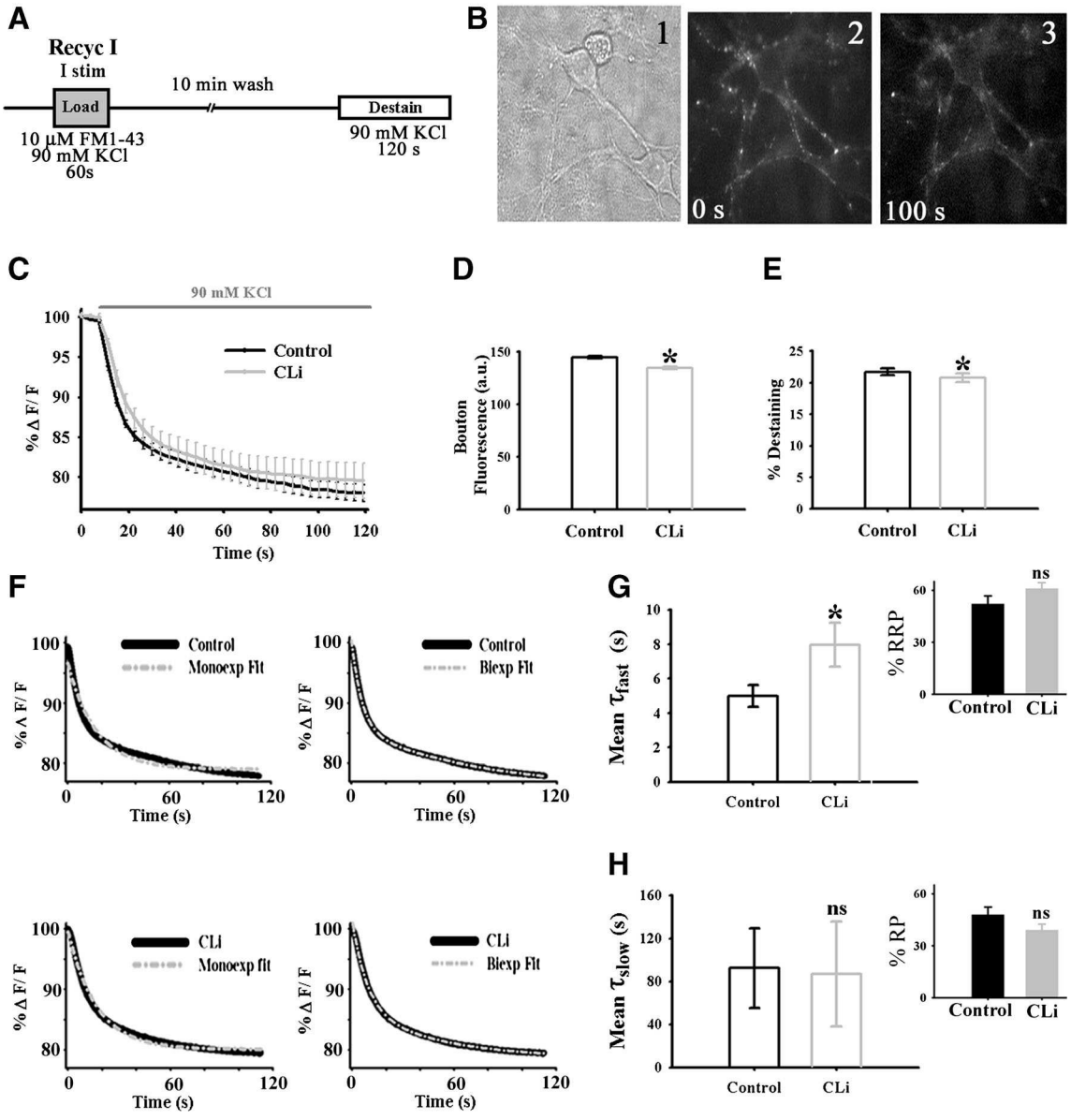

Figure 4. Boutons in lithium-treated cultures show a decrease in fluorescence, % destaining and destaining rates (Recyc I). (**A**) Protocol schema – neurons were loaded with 10 µM FM1-43 using 90 mM KCl modified tyrode solution (MT solution) for 60 s, (Recyc I) washed with normal external solution with 1 mM Advasep for 10 min and then destained with MT solution. (**B**) Bright field image (panel 1) of the FM1-43-loaded neurons shown as fluorescence images in panels 2 and 3. Boutons can be seen as bright puncta (panel 2) lining the neuronal membrane whose brightness reduces post stimulation (panel 3) (prior to stimulation, 0 s, and 100 s after application of destaining stimulus) in dissociated hippocampal mixed culture. (**C**) Destaining profile of control and lithium-treated cultures (CLi) boutons in presence of MT solution (Mean±SEM shown). (**D**) Fluorescence values of FM1-43-loaded boutons (10 µM FM1-43 in MT solution for 60 s (Recyc I), for control and CLi. (**E**) % Destaining in CLi boutons was significantly lower than control. (**F**) The destaining profiles in control (upper panel) and CLi (lower panel) could be fit best with bi-exponential decay curves giving two τ values (τ_{fast} and τ_{slow}). (**G**) τ_{fast} of destaining in CLi was significantly slower than control boutons while (**H**) τ_{slow} was not significantly different (**G** and **H** inset – % RRP and RP calculated from amplitude associated with τ_{fast} and τ_{slow}). (Data from 10 sister-sets of control and CLi, pooled data from 900 boutons; * significant at $p<0.05$ and ns (non-significant) at $p>0.05$ unpaired two-tailed *t*-test.)

4.97±0.63 s and mean τ_{slow} was 92.17±36.99 s (figure 4G and H). Destaining in CLi was significantly slower; τ_{fast} was 7.95+ .25 s; while τ_{slow} (86.61±48.96 s) was not significantly different for CLi (figure 4G and H). The time constants (5.6 s

and 139.1 s) obtained in this study for control cultures are in close agreement with the time constants reported by Mozhayeva *et al.* (2002). The slow time constant was attributed to release of vesicles from slowly mobilizable pool and the fast component to the readily releasable pool. In CLi, the τ_{fast} alone was affected. This can result from differences in RRP or decrease in full collapse mode of exocytosis. To verify the differences in RRP size, the amplitude associated with each τ was analysed. Amplitudes associated with τ_{fast} and τ_{slow} were similar in control and CLi-RRP and slow releasable component (RP) were not significantly different in control and CLi (% RRP was 52.09±4.61 % and 60.91 ±3.47% in control and CLi respectively) (figure 4G and H inset) (% RRP and RP calculated from amplitudes associated, paramters 'a' and 'c" in the biexponential fit equation (ii), with τ_{fast} and τ_{slow} with respect to total destaining). In summary, CLi boutons showed decrease in initial fluorescence and % destaining indicating decreased vesicle pool size. The proportion of RRP and RP was not affected but the rate of RRP release was. To verify differences in modes of exocytosis to account for slower rates of destaining, minimum loading and chlorpromazine treatment experiments were done (see supplementary information sections 1.2 and 1.3). Results from these experiments (supplementary figures 1.3 and 1.4) indicate that there was not much difference between control and CLi in the modes of exocytosis. However, endocytosis seems to be affected in CLi, chlorpromazine treatment affected bouton fluorescence to a greater extent in control than CLi (supplementary figure 1.4).

3.4 *CLi boutons do not show high KCl associated potentiation*

Repetitive depolarization pulses using high KCl has been used in earlier studies to understand activity dependent potentiation of vesicle recycling in neuronal cultures (Wang *et al.* 2001; Volmer *et al.* 2006). High KCl-induced potentiation has been associated with LTP through activation of PKC (Roisin *et al.* 1997; Volmer *et al.* 2006). In order to understand whether activity dependent potentiation of vesicle recycling is affected by CLi, we used the vesicular recycling II (Recyc II) protocol. In Recyc II protocol, the boutons were depolarized with 90 mM KCl MT for two minutes and then after a 5 min wash period, the boutons were loaded with 10 μM FM1-43 using 90 mM KCl MT and then after a consequent 10 min wash (as used for Recyc I experiment), they were checked for destaining using 90 mM KCl MT.

Control and CLi boutons responded differently to this Recyc II treatment. Recyc II control boutons showed a significantly higher initial fluorescence and % destaining, the control boutons had an average fluorescence of (in a.u.) 164.84±2.03 (figure 5C) an increase of 13.67 % over control Recyc I loading value. % destaining showed a 30% increase, it was 28.21±0.39 (figure 5D). Vesicular recycling II for CLi on the other hand did not show any difference in loading when compared to the Recyc I CLi boutons, 139.17±1.46 a.u. (3.13% increase over CLi I stimulation loading value) (figure 5C). The % destaining seen was also not significantly higher. % destaining seen was 20.45±0.40 (−1.58% change over CLi recycling 1) (figure 5D). The time constants for destaining in Recyc II was similar to Recyc I destaining in both, control and CLi cultures (figure 5E and F). Control Recyc II τ_{fast} was 5.22±0.95 s and τ_{slow} was 37.31±6.27 s while CLi Recyc II τ_{fast} was 7.05±1.52 s and τ_{slow} was 37.10±5.81 s.

3.5 *Hyperosmotic treatment boosts dye uptake and destaining in CLi*

The hyperosmotic treatment experiments were done to verify if boutons in lithium-treated cultures differed in the availability of readily releasable pool (RRP). In these experiments, FM1-43-loaded boutons (10 μM dye, 90 mM KCl MT for 60 s) at the end of 10 min wash period were exposed to 800 mOsm MT solution (Hyp exp) for 2 min and then imaged for destaining with 90 mM KCl MT. The unanticipated results obtained are discussed below.

Surprisingly, the CLi boutons showed an increase in both fluorescence intensity and also % destaining after the hyperosmotic exposure (figure 6C and D). Recyc I+Hyp exp CLi had the following fluorescence intensity 175.33 ±1.64 a.u. (29.93% increase) and % destaining 25.62±0.33 (23.29% increase). This observation held true for the Recyc II+Hyp exp case as well (supplementary figure 1.5).

Recyc I control boutons treated with hyperosmolar solution (Recyc I+ Hyp exp) had the fluorescence intensity of 145.63±1.46 a.u. (2.39% increase over Recyc I) (figure 6C). The % destaining was not significantly different 20.86±0.39 (−3.88% change over Recyc I) (figure 6D).

From these results, it appears that FM1-43 uptake is increased/ boosted with hyperosmolar treatment in CLi boutons due to activation of an endocytosis pathway that is probably different from CME (supplementary figure. 1.4). The increased destaining response, indicative of increased release, is probably due to an increase in the recycling pool size.

4. Discussion

4.1 *Effect of lithium on AMPAR mEPSCs*

It was found that long-term lithium treatment (CLi) caused a reduction in the mean mEPSC amplitudes, figure 1A. This is in agreement with the observations in earlier studies (Du *et al.* 2008). They found a reduction in surface expression of GluA1/2 upon treatment with lithium. The kinetics of the events was not significantly different from control. The

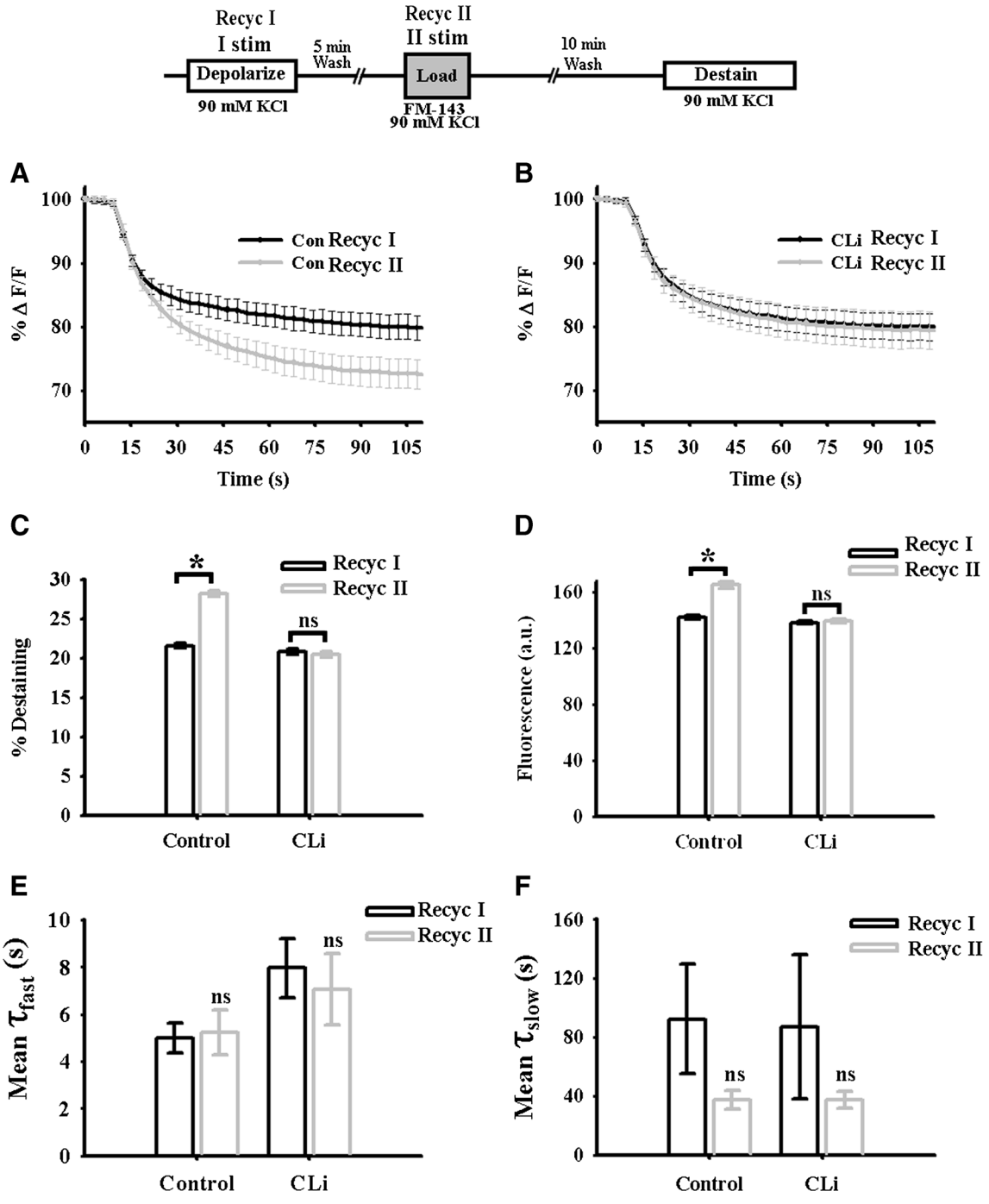

Figure 5. Control boutons loaded at Recyc II show increased fluorescence and destaining than CLi boutons. Protocol schema for II stimulation loading/Recyc II given on top (2 min, 90 mM KCl MT stimulus followed by loading with FM1-43 dye (10 μM in 90 mM KCl MT, 60 s). (**A**) Overlaid mean destaining profiles of control Recyc II and Recyc I FM1-43-loaded boutons; (**B**) overlaid mean destaining profiles of CLi Recyc II and Recyc I FM1-43 loaded boutons; (**C**) control boutons showed higher % destaining when loaded at II stimulus whereas change in CLi in Recyc-II-loaded boutons was not significantly different from CLi in Recyc-I-loaded boutons; (**D**) control boutons showed significantly higher fluorescence when loaded at Recyc II, whereas change is not significant in CLi boutons; (**E** and **F**) kinetics of destaining were not significantly different from Recyc-I-loading experiments (* significant at $p<0.05$ and ns (non-significant) at $p>0.05$ unpaired two-tailed *t*-test) (5 sister sets for control and CLi in Recyc II experiments; 500 boutons each).

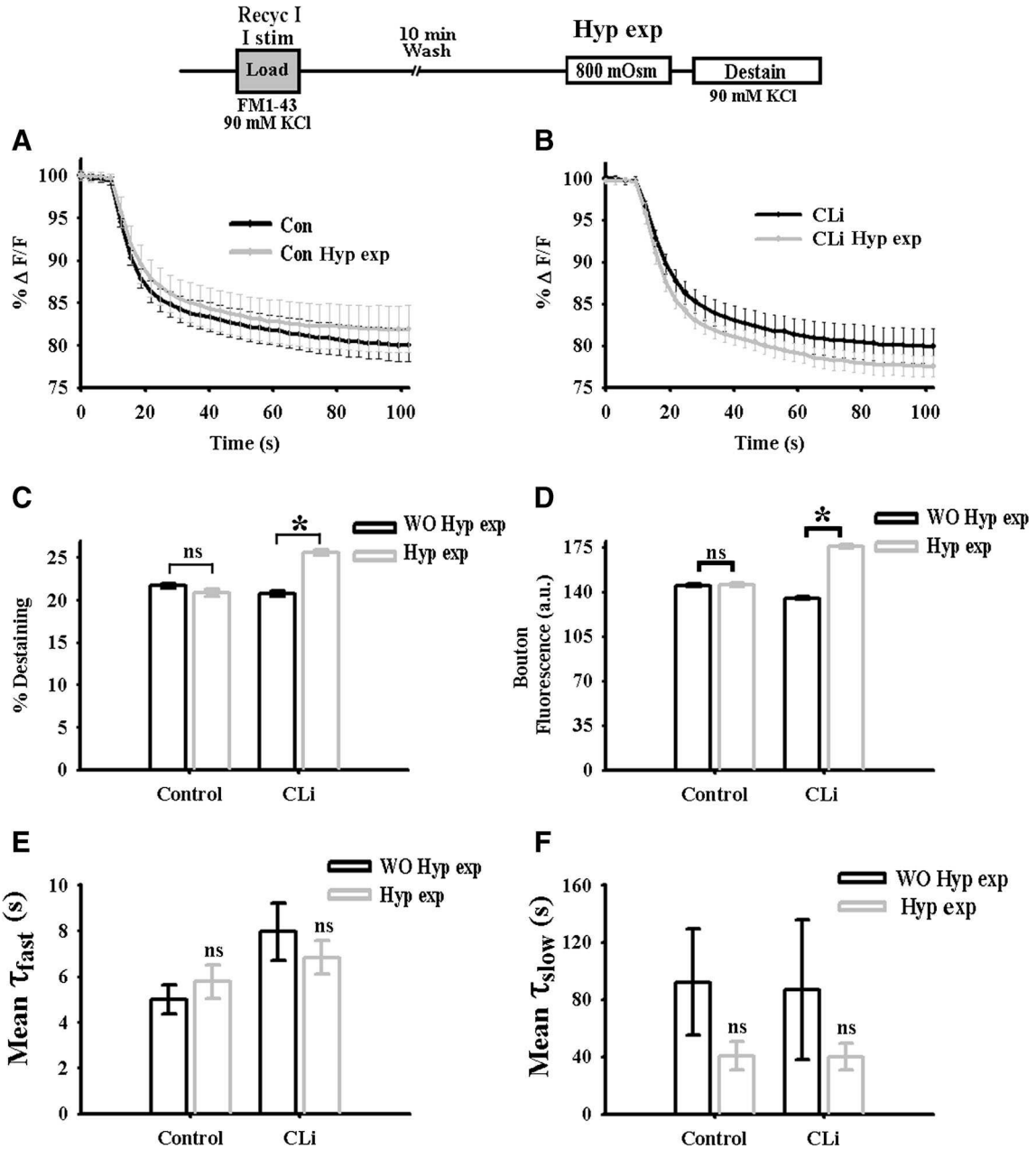

Figure 6. Lithium-treated boutons show significant enhancement in fluorescence and destaining when exposed to hypersosmotic solution as opposed to the control boutons (Recyc I+Hyp exp). Protocol schema given on top (destaining experiments were done after 2 min exposure to hyperosmotic solution). (**A**) Overlaid mean destaining profiles of control Recyc I FM1-43-loaded boutons with (Con Hyp exp) and without (Con) hyperosmotic stimulation; (**B**) overlaid mean destaining profiles of CLi I stimulus FM1-43-loaded boutons with (CLi Hyp exp) and without (CLi) hyperosmotic stimulation; (**C**) control boutons exposed to hyperosmotic solution (Hyp exp) showed destaining similar to control boutons which were not exposed to hyperosmotic solution (WO Hyp exp), whereas CLi boutons showed a significantly higher destaining than the ones not exposed to hyperosmotic solution; (**D**) fluorescence of CLi boutons was also significantly enhanced when exposed to hyperosmotic solution, fluorescence of control boutons was not affected; (**E** and **F**) kinetics of destaining were not significantly different from Recyc-I-loading experiments (* significant at $p<0.05$ and ns (non-significant_ at $p>0.05$ unpaired two-tailed *t*-test) (5 sister sets for control and CLi in Recyc I+Hyp exp experiments; 500 boutons each).

frequency of events in CLi was not statistically different. The mean RI of CLi was significantly reduced. This was not reported by Du *et al.* (2008). This could be either because of the difference in the age of cultures at the start of the lithium treatment or due to difference in technique used in both the studies. During early stages of development, most synapses have less AMPARs and more NMDARs (Lu *et al.* 2003). Insertion of AMPARs and their stabilization is an essential step in maturation of synapses (Ehlers 2000). AMPARs are tetrameric receptors. The four subunits of AMPAR, GluA1-4 combine in different combinations to form the functional receptors (Pellegrini-Giampietro *et al.* 1997). The expression of these subunits is developmentally regulated. GluA4 is highly expressed in the early phase of synapse development and its levels decrease during the later phases (Zhu *et al.* 2000). GluA1, GluA2 and GluA3 expression pick up slowly as the GluA4 levels drop. So the AMPAR subunit composition changes from GluA4/GluA4 to GluA1/GluA2 and GluA2/GluA3 (Zhu *et al.* 2000). This is reflected as a change in RI. This study was however done in hippocampal slice cultures. Thus the AMPARs change from being Ca^{2+}-permeable to Ca^{2+}-impermeable as GluA2-containing receptors are Ca^{2+}-impermeable. In the study presented here, higher mean RI was recorded in neurons from DIV 10-15 control cultures. In CLi cultures, neurons showed lowered mean RI in cultures of the same age (DIV10-15). Thus, it is possible that lithium interferes with progressive change in AMPAR subunits seen during maturation of synapses. The results from NASPM and DFMO experiments support the possibility that contribution of Ca^{2+}-permeable channels in synaptic events in CLi neurons is higher than in control neurons. Further experiments are needed to understand this effect of lithium on AMPARs.

Experiments done to elucidate molecular players involved in modulating AMPAR mEPSCs revealed that co-inhibiting PKA, GSK-3β and glutamate reuptake is required to closely reproduce the effects of CLi on AMPAR mEPSCs (figure 7) (and see supplementary section 2 for experimental details on inhibiting PKA, GSK-3β and glutamate reuptake individually and in various combinations). When similarity across all the mEPSC parameters were checked for the changes induced by drug treatments with those induced by lithium treatment, it was found that with respect to mean RI two groups emerged- Group I showing decreased RI similar to CLi and Group II in which the RI was not decreased (figure 7B, C and D). Group I treatments consisted of THA acute, SB, THA+SB and THA+H89+SB (figure 7C). Among these THA+H89+SB seemed to be most similar to CLi except for frequency of mEPSCs (amplitude was not as low in CLi, but significantly lower than control). SB also had many similarities with CLi induced changes but the τ_{decay} was significantly slower (than that in CLi) (figure 7C). Also, the very high amplitude events seen in SB (supplementary figure 2.2B*) were not present in CLi. Group II had H89, H89+SB, THA, THA+H89 treatments. These had mean RI greater than that of CLi (similar to control value or even greater). The decrease in mEPSC amplitude was seen in all the treatment groups. Data from multiple inhibition results presented here suggest that in order to mimic the effect of lithium fully, many molecules in the system may have to be perturbed, underscoring the point that lithium is a broad-spectrum inhibitor.

4.2 *Effect of lithium on vesicle recycling*

In this study it was found that I stimulation loaded boutons (vesicle recycling I (Recyc I)) in CLi cultures showed lower dye uptake, lower % destaining and slower kinetics of destaining (figure 4D, E and G). Minimum loading experiments did not show any differences in the % of boutons undergoing multistep destaining (supplementary figure 1.3C). % destaining and rate of destaining in control and CLi was affected to similar extent upon chlorpromazine treatment (supplementary figure 1.4C and E). RRP availability was also not different in CLi (figure 4G inset). Lithium is known to inhibit PKA and PKC which in turn modulate the activity of proteins which are known to be involved in docking and priming steps (Mori *et al.* 1996; Wang *et al.* 2001; Leenders and Sheng 2005). The slow rate of dye loss seen in CLi may be due to differences in vesicle mobilization for release rather than a change in mode of exocytosis. Further experiments are needed to confirm this.

When loaded during second round of recycling (Recyc II), control boutons showed enhanced fluorescence and destaining (figure 5C and D). The enhancement in fluorescence and destaining, seen in control boutons when they were loaded during vesicle recycling II, was absent post exposure to hyperosmotic solution (supplementary figure 5C and D), indicating that the increase seen was due to enhanced RRP size. Hippocampal neurons are capable of maintaining sustained release even in the presence of prolonged strong stimulus (Sara *et al.* 2002). A fast mode of endocytosis is activated in such conditions and helps in maintaining the sustained response. This mode of endocytosis replenishes RRP (Sara *et al.* 2002). The increased fluorescence, seen post loading during vesicle recycling II in control in this study, may be because of the activation of this fast mode of endocytosis due to the application of the strong stimulus. Application of high KCl solution (50 mM, 40 s) has been shown to bring about PKC (γ-isoform) mediated LTP in hippocampal slices (Roisin *et al.* 1997). Presynaptic release has been shown to increase on application of two consecutive pulses of high KCl solution separated by 5 min (Volmer *et al.* 2006), quite similar to the protocol used in our experiments. PKC activity has been implicated in this effect. Whether the increase in fluorescence and destaining seen

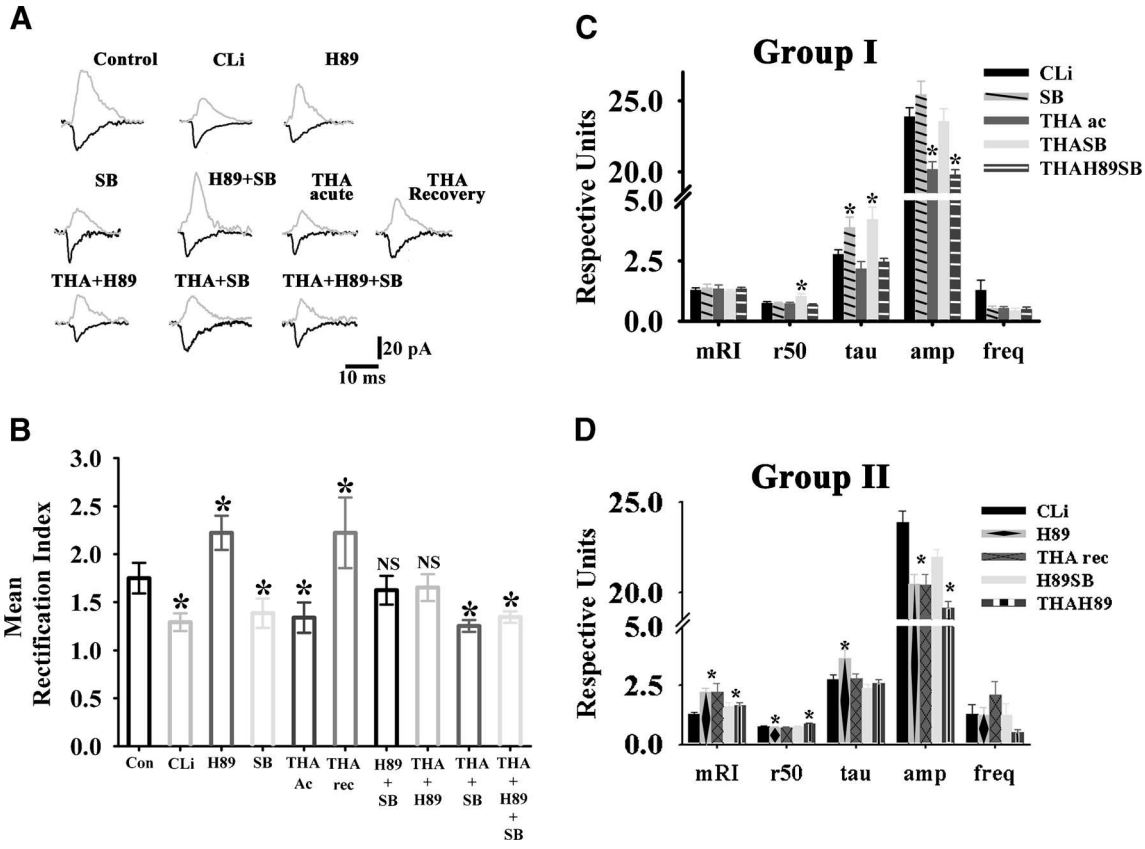

Figure 7. Comparison of changes induced in parameters across different treatment groups. (**A**) Overlay of average mEPSCs in neurons, for all the treatment protocols used, at −70 mV and +50 mV holding voltages (black trace for −70 mV and gray for +50 mV); (**B**) the mean RI for all the treatment groups, notice that SB (SB415286-treated (GSK-3β inhibited), THA+SB ((or THASB)− THA-treated cultures maintained in SB415286) and THA+H89+SB ((or THAH89SB)− THA-treated cultures maintained in H-89 and SB415286) have decreased mean RI (mRI); (**C**) the groups showing lowered mean RI are compared with CLi for similarities in changes, notice that THA+SB differs significantly from CLi in half rise time (r50) and τ_{decay} (tau) (slower kinetics, statistically significant indicated by *), whereas the SB differs in τ_{decay}; THA+SB+H89 differs only in amplitude which is significantly lower than CLi. Changes in frequency were not similar to that seen in CLi but they were also not significantly different; (**D**) the group with significantly higher mean RI than CLi (* significant at $p<0.05$ by ANOVA, Kruskal–Wallis test). Abbreviations used: CLi, lithium-treated; H89, H-89-treated (PKA inhibited); SB, SB415286-treated (GSK-3β inhibited); THA ac, (THA acute) 24 h THA treatment on DIV 10; THA rec, (THA recovery) 24 h THA treatment on DIV 4; H89+SB (or H89SB), H-89 and SB415286-treated; THA+H89 (or THAH89), THA-treated cultures maintained in H-89; THA+SB (or THASB), THA-treated cultures maintained in SB415286; THA+H89+SB ((or THAH89SB), THA-treated cultures maintained in H-89 and SB415286; mRI, mean rectification index; r50, half rise time (in ms); tau, decay time constant τ_{decay} (in ms); amp, mean mEPSC amplitude (in pA); freq, frequency of events (in Hz) (kinetics, amplitude and frequency of events as measured at −70 mV holding voltage). (See supplementary section 2.3 for experimental details and number of neurons used for analysis).

here is attributable to such a LTP induction or due to activated fast endocytosis is not clear from our experiments, further experiments are needed to verify these possibilities. Interestingly, in CLi boutons such a potentiation was absent (figure 5D). Lithium is known to inhibit PKC (Wang *et al.* 2001).

The unexpected and surprising results of hyperosmotic exposure experiments discussed below throw up a possibility for existence of a disrupted form of endocytosis in CLi boutons. CLi boutons showed enhanced fluorescence and % destaining upon exposure to hyperosmotic MT given 10 min post dye wash out. Hence, this increase in fluorescence of boutons in the absence of dye in external solution indicates that FM1-43 is still available for internalization 10 min after dye wash out, in other words FM1-43 is trapped away from external solution. FM1-43 dye has the property of being trapped in membrane infoldings and as such, FM1-43 stains vesicles retrieved by bulk endocytosis better (Richards *et al.* 2000). Bulk endocytosis has been shown to complete

within the span of applied strong stimulus (Clayton *et al.* 2008). Since hyperosmotic exposure was given after a long delay and was still able to boost dye uptake indicates that the CLi boutons have a compromised form of endocytosis with formation of membranous infoldings (figure 8B). The percent enhancement in fluorescence and destaining in response to hyperosmotic exposure given post vesicle recycling II dye loading is lower (as compared to Recyc I+Hyp exp), supporting the possibility of a compromised endocytosis in CLi (figure 8A).

Compromised endocytosis with membrane infoldings have been documented in dynamin knockout experiments. Dynamin-I knockout lead to massive accumulation of interconnected clathrin-coated buds which are accessible to extracellular tracers indicating impaired fission of pits (Ferguson *et al.* 2007). Lithium treatment could modulate dynamin by inhibiting GSK-3β (Phiel and Klein 2001) or the long-term treatment might lead to changes in dynamin expression. GSK-3β modulates activity dependent bulk endocytosis by modulating dynamin-I through phosphorylation (Clayton *et al.* 2010). Dynamin has three isoforms (Clayton and Cousin 2009). In absence of dynamin I other forms of dynamin are known to help in vesicle retrieval, especially dynamin-III (Ferguson *et al.* 2007; Clayton and Cousin 2009). It would be interesting to see if expression of the dynamin-I and its other forms are altered in lithium exposed developing hippocampal neurons.

In summary, the initial fluorescence of boutons and % destaining in response to high KCl stimulation is lower in lithium-treated cultures. Therefore, it can be concluded that lithium brings about a decrease in recycling pool size. This decrease in recycling pool is rescued (or rather recycling pool is boosted) by application of hyperosmotic solution. Dye uptake in lithium-treated cultures is also resilient to disruption of clathrin-mediated endocytosis (CME) (chlorpromazine treatment). Destaining was also slower in lithium-

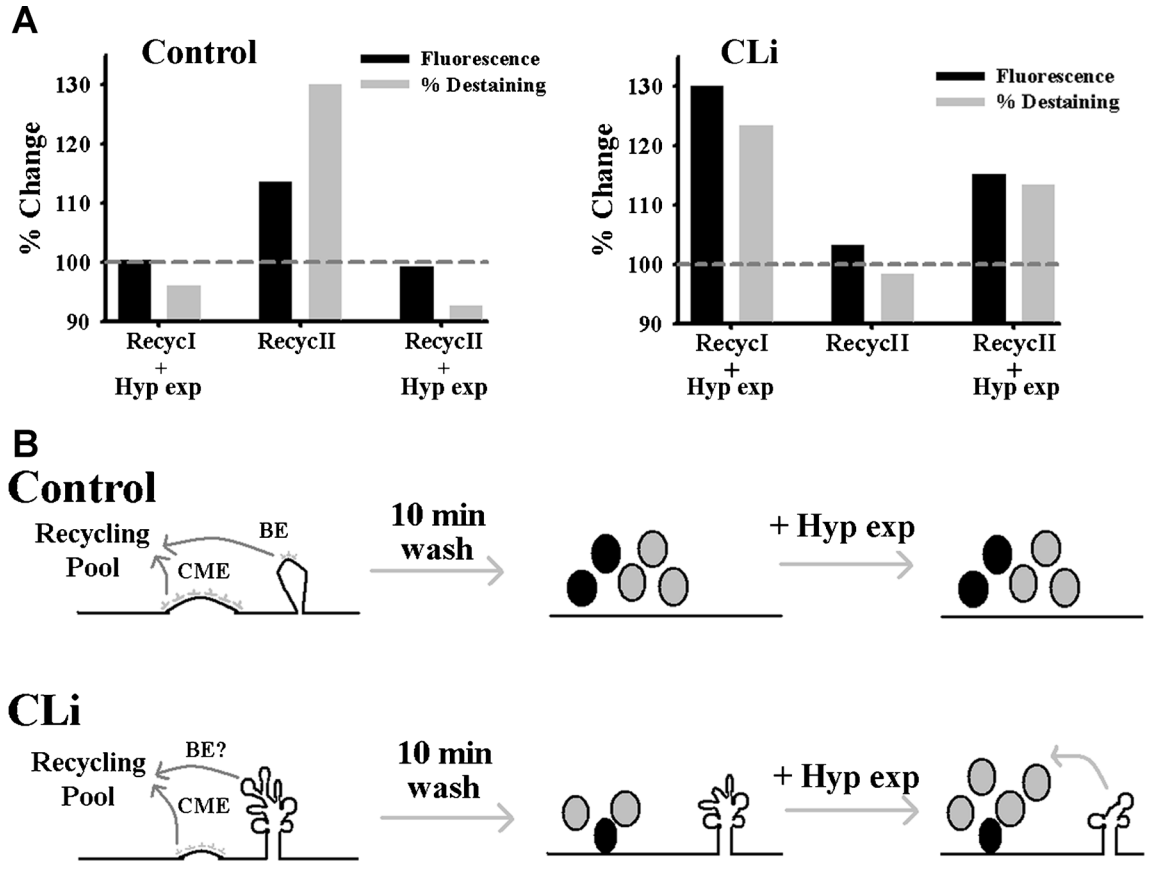

Figure 8. Effect of lithium treatment on vesicular endocytosis and exocytosis. (**A**) Percentage changes were calculated with respect to Recyc I values in control and CLi respectively and 100 % represents no change in both the cases with respect to Recyc I values. (**B**) Endocytosis cartoon summarizing the effect of CLi; Vesicular endocytosis in CLi is compromised. Dependence on clathrin mediated endocytosis (CME) is low; endocytosis may progress through membrane infoldings similar to bulk endocytosis (BE) (indicated by question mark) but stalled at fission step (exposure to hyperosmotic solution rescues and boosts endocytosis allowing dye trapped in budding vesicles to contribute to the recycling pool). Vesicles formed from CME are represented as black and from BE as grey filled circles.

treated cultures. Thus lithium treatment from DIV 4-10, affects vesicular release and recycling. Presynaptic potentiation seen upon repeated application of high KCl was also absent in lithium-treated cultures. This is the first study to report the effect of prolonged lithium exposure during synaptogenesis on presynapse.

5. Conclusion

In this study involving cultures from normal rat pups it was found that lithium exposure (1 mM, from DIV 4-10) during synapse development affects both the pre and the postsynapse. The rectifying AMPAR mEPSCs are signatures of Ca^{2+}-permeable AMPARs that have been implicated in neuropathological conditions (Van Den Bosch *et al.* 2000; Weiss and Sensi 2000, Lee *et al.* 2002, Noh *et al.* 2005). The amplitudes of AMPAR mEPSCs are also reduced. AMPARs are necessary for normal physiological functioning of the glutamatergic synapses mostly in learning and memory formation (Zarate and Manji 2008). The same treatment also affected the vesicle pool mobilization and endocytosis. Lithium treatment also inhibited high KCl-induced presynaptic potentiation. Thus, the present study might have implications in understanding the cases of perinatal and neonatal exposure to lithium (Morrell *et al.* 1983; Newport *et al.* 2005; Kent 2008) and cognitive dulling in patients on lithium therapy (Dunner 2000).

In conclusion, chronic lithium treatment affected both the presynaptic and postsynaptic compartments of the glutamatergic synapse. The effect of lithium on AMPAR mEPSC could not be reproduced by individual inhibitions of biochemical effectors but by co-inhibition of three enzymes. Thus, the study done here underscores the need to look at the manifold effect of lithium in an integrated way.

Acknowledgements

We would like to acknowledge Council of Scientific and Industrial Research (CSIR), India, for extending financial support in the form of CSIR fellowship to SMA.

References

Akaneya Y, Sohya K, Kitamura A, Kimura F, Washburn C, Zhou R, Ninan I, Tsumoto T, *et al*. 2010 Ephrin-A5 and EphA5 interaction induces synaptogenesis during early hippocampal development. *PLoS One* **5** 1–20

Bonanomi D, Menegon A, Miccio A, Ferrari G, Corradi A, Kao H-T, Benfenati F and Valtorta F 2005 Phosphorylation of synapsin I by cAMP-dependent protein kinase controls synaptic vesicle dynamics in developing neurons. *J. Neurosci.* **25** 7299–7308

Chen G, Rajkowska G, Du F, Seraji-Bozorgzad N and Manji HK 2000 Enhancement of hippocampal neurogenesis by lithium. *J. Neurochem.* **75** 1729–1734

Clayton EL and Cousin MA 2009 The molecular physiology of activity-dependent bulk endocytosis of synaptic vesicles. *J. Neurochem.* **111** 901–914

Clayton EL, Evans GJO and Cousin MA 2008 Bulk synaptic vesicle endocytosis is rapidly triggered during strong stimulation. *J. Neurosci.* **28** 6627–6632

Clayton EL, Sue N, Smillie KJ, O'Leary T, Bache N, Cheung G, Cole AR, Wyllie DJ, *et al*. 2010 Dynamin I phosphorylation by GSK3 controls, activity-dependent bulk endocytosis of synaptic vesicles. *Nat. Neurosci.* **13** 845–853

Cohen-Cory S 2002 The developing synapse: construction and modulation of synaptic structures and circuits. *Science.* **298** 770–776

Cottrell JR, Dube GR, Egles C and Liu G 2000 Distribution, density, and clustering of functional glutamate receptors before and after synaptogenesis in hippocampal neurons. *J. Neurophysiol.* **84** 1573–1587

Du J, Creson TK, Wu L-J, Ren M, Gray NA, Falke C, Wei Y, Wang Y, *et al*. 2008 The role of hippocampal GluR1 and GluR2 receptors in manic-like behavior. *J. Neurosci.* **28** 68–79

Dunner DL 2000 Optimising lithium treatment. *J. Clin. Pscychiatry.* **61** 76–81

Ehlers MD 2000 Reinsertion or Degradation of AMPA Receptors determined by activity-dependent endocytic sorting. *Neuron.* **28** 511–525

Ferguson SM, Brasnjo G, Hayashi M, Wölfel M, Collesi C, Giovedi S, Raimondi A, Gong L-W, *et al*. 2007 Selective activity-dependent requirement for dynamin 1 in synaptic vesicle endocytosis. *Science* **316** 570–574

Gilad GM, Gilad VH and Casero RA Jr 1994 Lithium exerts a time-dependent and tissue-selective attenuation of the dexamethasone-induced polyamine response in rat brain and liver. *Brain Res.* **636** 187–192

Gilad GM and Gilad VH 2007 Astroglia growth retardation and increased microglia proliferation by lithium and ornithine decarboxylase inhibitor in rat cerebellar cultures: Cytotoxicity by combined lithium and polyamine inhibition. *J. Neurosci. Res.* **85** 594–601

Hashimoto R, Hough C, Nakazawa T, Yamamoto T and Chuang D-M 2002 Lithium protection against glutamate excitotoxicity in rat cerebral cortical neurons: involvement of NMDA receptor inhibition possibly by decreasing NR2B tyrosine phosphorylation. *J. Neurochem.* **80** 589–597

Iqbal Z 1995 Excitatory amino acid receptor-mediated neuronal signal transduction: modulation by polyamines and calcium. *Mol. Cell. Biochem.* **149** 233–240

Kent A 2008 Psychiatric disorders in pregnancy. *Obstet. Gynaecol. Reprod. Med.* **19** 37–41

Koike M, Iino M and Ozawa S 1997 Blocking effect of 1-naphthyl acetyl spermine on Ca^{2+}-permeable AMPA receptors in cultured rat hippocampal neurons. *Neurosci. Res.* **29** 27–36

Kugaya A and Sanacora G 2005 Beyond monoamines: Glutamatergic function in mood disorders. *CNS Spectr.* **10** 808–819

Lee AL, Ogle WO and Sapolsky RM 2002 Stress and depression: possible links to neuron death in the hippocampus. *Bipolar Disord.* **4** 117–128

Leenders AGM and Sheng Z-H 2005 Modulation of neurotransmitter release by the second messenger-activated protein kinases: Implications for presynaptic plasticity. *Pharmacol. Therapeut.* **105** 69–84

Lenox RH and Wang L 2003 Molecular basis of lithium action: integration of lithium-responsive signaling and gene expression networks. *Mol. Psychiat.* **8** 135–144

Loepke AW, McGowan FX Jr and Soriano SG 2008 CON: The toxic effects of anesthetics in the developing brain: The clinical perspective. *Int. Anesth. Res. Soc.* **106** 1664–1669

Lu H-C, She W-C, Plas DT, Neumann PE, Janz R and Crair MC 2003 Adenylyl cyclase I regulates AMPA receptor trafficking during mouse cortical 'barrel' map development. *Nat. Neurosci.* **6** 939–942

Manji HK, Drevets WC and Charney DS 2001 The cellular neurobiology of depression. *Nat. Med.* **7** 541–547

Mori S, Zanardi R, Popoli M, Smeraldi E, Racagni G and Parez J 1996 Inhibitory effect of lithium ion on cAMP dependent phosphorylation system. *Life Sci.* **59** PL 99–104

Morrell P, Sutherland GR, Buamah Moo PK and Bain HH 1983 Lithium toxicity in a neonate. *Arch. Dis. Child.* **58** 539–541

Mozhayeva MG, Sara Y, Liu X and Kavalali ET 2002 The Development of Vesicle Pools during Maturation of Hippocampal Synapses. *J. Neurosci.* **22** 654–665

Newport DJ, Viguera AC, Beach AJ, Ritchie JC, Cohen LS and Stowe ZN 2005 Lithium placental passage and obstetrical outcome: Implications for clinical management during late pregnancy. *Am. J. Psychiatry.* **162** 2162–2170

Noh K-M, Yokota H, Mashiko T, Castillo PE, Zukin RS and Bennett VLM 2005 Blockade of calcium-permeable AMPA receptors protects hippocampal neurons against global ischemia-induced death. *Proc. Natl. Acad. Sci. USA* **102** 12230–12235

Nonaka S, Hough CJ and Chuang D-M 1998 Chronic lithium treatment robustly protects neurons in the central nervous system against excitotoxicity by inhibiting N-methyl-D-aspartate receptor-mediated calcium influx. *Proc. Natl. Acad. Sci. USA* **95** 2642–2647

Pellegrini-Giampietro DE, Gorter JA, Bennett MVL and Zukin RS 1997 The GluR2 (GluR-B) hypothesis: Ca^{2+}-permeable AMPA receptors in neurological disorders. *Trends Neurosci.* **20** 464–470

Phiel CJ and Klein PS 2001 Molecular targets of lithium action. *Ann. Rev. Pharmacol. Toxicol.* **41** 789–813

Rao SP and Sikdar SK 2004 Estradiol-induced changes in the activity of hippocampal neurons in network culture are suppressed by co-incubation with gabapentin. *Brain Res.* **1022** 126–136

Richards DA, Guatimosim C and Betz WJ 2000 Two endocytic recycling routes selectively fill two vesicle pools in frog motor nerve terminals. *Neuron.* **27** 551–559

Roisin M-P, Leinekugel X and Tremblay E 1997 Implication of protein kinase C in mechanisms of potassium- induced long-term potentiation in rat hippocampal slices. *Brain Res.* **745** 222–230

Sara Y, Mozhayeva MG, Liu X and Kavalali ET 2002 Fast Vesicle Recycling Supports Neurotransmission during Sustained Stimulation at Hippocampal Synapses. *J. Neurosci.* **22** 1608–1617

Shin J, Shen F and Huguenard JR 2005 Polyamines modulate AMPA receptor-dependent synaptic responses in immature layer V pyramidal neurons. *J. Neurophysiol.* **93** 2634–2643

Sjöholm A, Welsh N and Hellerström C 1992 Lithium increases DNA replication, polyamine content, and insulin secretion by rat pancreatic beta-cells. *Am. J. Physiol.* **262** C391–5

Sparapani M, Virgili M, Ortali F and Contestabile A 1997 Effects of chronic lithium treatment on ornithine decarboxylase induction and excitotoxic neuropathology in the rat. *Brain Res.* **765** 164–168

Speese SD and Budnik V 2007 Wnts: Up-and-coming at the synapse. *Trends Neurosci.* **30** 268–275

Srinivas KV, Jain R, Saurav S and Sikdar SK 2007 Small-world network topology of hippocampal neuronal network is lost, in an in vitro glutamate injury model of epilepsy. *Eur. J. Neurosci.* **25** 3276–3286

Van Den Bosch L, Vandenberghe W, Klaassen H, Van Houtte E and Robberecht W 2000 Ca^{2+}-permeable AMPA receptors and selective vulnerability of motor neurons. *J. Neurol. Sci.* **180** 29–34

van den Pol AN, Obrietan K, Belousov AB, Yang Y and Heller HC 1998 Early Synaptogenesis *In Vitro*: Role of Axon Target Distance. *J. Comp. Neurol.* **399** 541–560

Volmer R, Monnet C and Gonzalez-Dunia D 2006 Borna Disease Virus Blocks Potentiation of Presynaptic Activity through Inhibition of Protein Kinase C Signaling. *PLoS Pathog.* **2** e19

Wang H-Y, Johnson GP and Friedman E 2001 Lithium treatment inhibits protein kinase C translocation in rat brain cortex. *Psychopharmacology.* **158** 80–86

Weiss JH and Sensi SL 2000 Ca^{2+}-Zn^{2+} permeable AMPA or kainate receptors: possible key factors in selective neurodegeneration. *Trends Neurosci.* **23** 365–371

Wierenga CJ, Ibata K and Turrigiano GG 2005 Postsynaptic expression of homeostatic plasticity at neocortical synapses. *J. Neurosci.* **25** 2895–2905

Zarate CA Jr and Manji HK 2008 The Role of AMPA Receptor modulation in the treatment of neuropsychiatric diseases. *Exp. Neurol.* **211** 7–10

Zhu JJ, Esteban JA, Hayashi Y and Malinow R 2000 Synaptic potentiation during early development: delivery of GluR4-containing AMPA receptors by spontaneous activity. *Nat. Neurosci.* **3** 1098–1106

MS received 01 October 2014; accepted 23 March 2015

Corresponding editor: NEERAJ JAIN